

Crossed Andreev reflection in collinear p -wave magnet-triplet superconductor junctions

Abhiram Soori*

School of Physics, University of Hyderabad, Prof. C. R. Rao Road, Gachibowli, Hyderabad-500046, India

Crossed Andreev reflection (CAR) is a fundamental quantum transport phenomenon with significant implications for spintronics and superconducting devices. However, its experimental detection and enhancement remain challenging. In this work, we propose a junction comprising p -wave magnets and a triplet superconductor as a promising platform to enhance CAR. The setup features a triplet superconductor sandwiched between two collinear p -wave magnets, rotated by 180° relative to one another, enabling precise control of transport processes. We show that CAR can dominate over electron tunneling (ET) for specific parameter regimes, such as the orientation angle of the p -wave magnets and the chemical potential. Enhanced CAR is achieved when the constant energy contours of the two spins in the p -wave magnets are well-separated. Additionally, the conductivities exhibit Fabry-Pérot-type oscillations due to interference effects, with CAR diminishing as the superconductor length exceeds the decay length of the wavefunctions. These findings highlight the potential of collinear p -wave magnet-superconductor junctions as a robust platform for the experimental study and enhancement of CAR.

Introduction .- The concept of altermagnetism has drawn significant attention from theorists and experimentalists in recent years [1–4]. Altermagnets can be regarded as the magnetic analogs of d -wave superconductors. While the magnetic counterparts of p -wave superconductors are spin-orbit-coupled materials, the magnetic equivalent of the anisotropic triplet pairing observed in liquid He-3 is the p -wave magnet [5–9].

Unlike d -wave altermagnets, p -wave magnets preserve time-reversal symmetry. Although p -wave magnets share qualitative similarities with spin-orbit-coupled systems, their bandstructure is highly anisotropic when viewed from $\vec{k} = 0$ (see Fig. 1). In two dimensions, spin-orbit coupling introduces a term proportional to $(\sigma_x k_y - \sigma_y k_x)$ in the Hamiltonian, whereas p -wave magnets are characterised by the term $\sigma_z k_x$, which leads to the anisotropic Fermi surface. Both d -wave altermagnets and p -wave magnets exhibit zero net spin polarisation. However, a voltage-biased junction of d -wave altermagnets with metals has been shown to carry a spin current [10], and a similar biased junction between p -wave magnets and metals generates a transverse spin current [7].

Andreev reflection is a fundamental process at the interface between a superconductor and another material, where an incoming electron is reflected as a hole, forming a Cooper pair in the superconductor [11]. In altermagnet-superconductor junctions, maximal Andreev reflection occurs for specific orientations of the altermagnet due to its spin-split band structure [12, 13]. However, for p -wave magnets, the preserved time-reversal symmetry ensures that the constant energy contours in \vec{k} -space for electrons and holes with opposite spins are closely aligned (see Fig. 2), enabling Andreev reflection regardless of the p -wave magnet's orientation relative to the superconductor [14]. When the superconductor has triplet pairing, the situation changes: Andreev reflection involves electrons and holes of the same spin, making the spin-split

band structure of the p -wave magnet critical in determining the orientations that allow Andreev reflection.

Crossed Andreev reflection (CAR) is an extension of this phenomenon, where the incoming electron and outgoing hole lie in different regions of the system, such as distinct p -wave magnets in contact with a superconductor. CAR has been widely studied in junctions involving normal metals, ferromagnets, altermagnets, and superconductors [15–24]. It has been proposed as a tool for detecting superconducting pairing symmetry [25, 26]. Also, it has garnered interest as the inverse process of Cooper pair splitting wherein two nonlocally entangled electrons can be produced [27–29]. However, experimental observations of CAR remain limited [15, 30] because electron tunnelling (ET) through the superconductor often dominates over CAR.

In this work, we study electron transport in a junction comprising two p -wave magnets and a triplet superconductor using Landauer-Büttiker scattering theory, focusing on the interplay between CAR and ET. We show that when the orientations of the two p -wave magnets are rotated by 180° and lie within a specific range of directions, CAR dominates over ET. Under these conditions, ET does not contribute to the current, providing a unique regime where CAR can be isolated and controlled. This finding highlights the potential of p -wave magnet-superconductor junctions for achieving enhanced control over CAR.

System and Key Result.— We consider a junction where p -wave magnets are attached on either side of a triplet superconductor, with the p -wave magnet on the right rotated by 180° relative to the one on the left. Fig. 2(a) and Fig. 2(b) illustrate the constant energy contours of the dispersion relations for the two p -wave magnets. These figures reveal that the transverse wavenumber k_y in a range matches across the junction for electrons on the left and holes on the right, both having same spin.

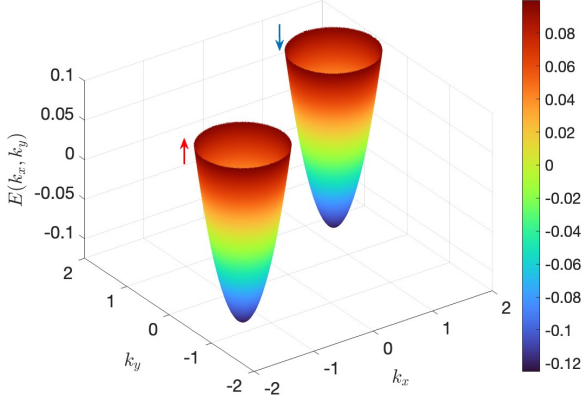


FIG. 1. Bandstructure of a p -wave magnet.

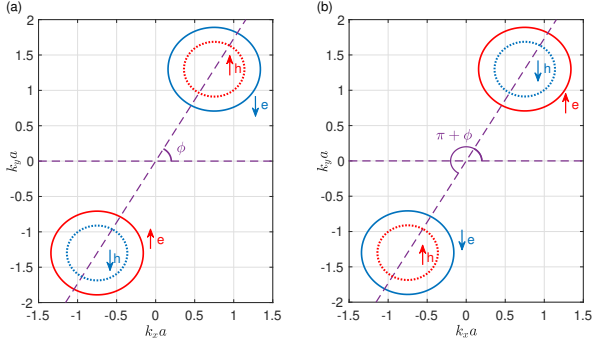


FIG. 2. Constant energy contours of the left (a) and right (b) p -wave magnets. Note that k_y of electrons and holes of the same spin on either sides match in a certain range, giving scope for CAR. Parameters: $\mu = -\mu_s$, $\alpha = 1.5\hbar m/a$, $\phi = \pi/3$ and $E = 0.05\mu_s$.

Due to this, incident electrons from the left p -wave magnet scatter into hole states on the right, provided equal spin electron-to-hole conversion occurs in the central superconducting region. This conversion is facilitated by the triplet pairing in the superconductor.

Hamiltonian. - The Hamiltonian for the system is given by

$$H = \begin{cases} \left[\frac{-\hbar^2 \vec{\nabla}^2}{2m} - \mu \right] \tau_z \sigma_0 - i\alpha \hbar (\hat{n}_\phi \cdot \vec{\nabla}) \tau_0 \sigma_z, & \text{for } x < 0, \\ \left[\frac{-\hbar^2 \vec{\nabla}^2}{2m} - \mu_s \right] \tau_z \sigma_0 - \frac{i\hbar \Delta \partial_x}{k_F} \tau_x \sigma_\theta, & \text{for } 0 < x < L, \\ \left[\frac{-\hbar^2 \vec{\nabla}^2}{2m} - \mu \right] \tau_z \sigma_0 - i\alpha \hbar (\hat{n}_{\pi+\phi} \cdot \vec{\nabla}) \tau_0 \sigma_z, & \text{for } x > L, \end{cases} \quad (1)$$

where m is the effective mass of electrons, μ (μ_s) is the chemical potential in the p -wave magnet (superconductor), and α is the strength of the p -wave magnet term. The unit vector $\hat{n}_\phi = (\cos \phi \hat{x} + \sin \phi \hat{y})$ makes

an angle ϕ with \hat{x} . The Pauli matrices τ_j and σ_j act on the particle-hole and spin sectors, respectively, with $j = 0, x, y, z$. Here, $\vec{\nabla} = \hat{x}\partial_x + \hat{y}\partial_y$, $k_F = \sqrt{2m\mu_s/\hbar^2}$, and $\sigma_\theta = \cos \theta \sigma_z + \sin \theta \sigma_x$, where θ is the angle made by the spin direction of the equal-spin triplet pairing in the superconductor with \hat{z} , the easy axis of the p -wave magnet. The length of the central superconducting region is L . The Hamiltonian acts on the four-spinor $\Psi = [\psi_{e,\uparrow}, \psi_{e,\downarrow}, \psi_{h,\uparrow}, \psi_{h,\downarrow}]^T$, where subscripts denote particle type and spin.

A voltage bias V is applied from the left p -wave magnet, with the superconductor and the right p -wave magnet grounded. The currents I_L and I_R in the left and right regions, and the differential conductances $G_{\mathcal{L}\mathcal{L}} = dI_{\mathcal{L}}/dV$ and $G_{\mathcal{R}\mathcal{L}} = dI_{\mathcal{R}}/dV$ are calculated.

Dispersion. - The dispersion relation in the p -wave magnet is given by

$$E = \eta_p \left[\frac{\hbar^2 (k_x^2 + k_y^2)}{2m} - \mu \right] + \gamma \eta_s \alpha \hbar (\cos \phi k_x + \sin \phi k_y), \quad (2)$$

where $p = e, h$ denotes electrons or holes, $s = \uparrow, \downarrow$ denotes the spin, $\eta_{e/h} = \pm 1$, $\eta_{\uparrow/\downarrow} = \pm 1$, and $\gamma = 1$ (-1) for $x < 0$ ($x > L$). The opposite signs of γ in $x < 0$ and $x > L$ reflect the 180° rotation of the p -wave magnets relative to one another. A typical dispersion relation is plotted in Fig. 1. The wavenumbers k_x and k_y for a given energy E are parametrized as

$$\begin{aligned} k_x(p, E, \chi) &= k_{0,p} \cos \chi - \gamma \eta_s \eta_p \alpha m \cos \phi / \hbar, \\ k_y(p, E, \chi) &= k_{0,p} \sin \chi - \gamma \eta_s \eta_p \alpha m \sin \phi / \hbar, \end{aligned} \quad (3)$$

where $k_{0,p} = \sqrt{(\alpha m / \hbar)^2 + 2m(\mu + \eta_p E) / \hbar^2}$, and χ is the angle of the velocity vector relative to \hat{x} .

The dispersion relation in the superconductor is given by

$$E = \pm \sqrt{\left[\frac{\hbar^2 (k_x^2 + k_y^2)}{2m} - \mu_s \right]^2 + \frac{k_x^2}{k_F^2} \Delta^2}. \quad (4)$$

Boundary Conditions. - To solve the scattering problem, boundary conditions are required in addition to the Hamiltonian in each region. The following boundary conditions ensure the conservation of probability current:

$$\begin{aligned} \Psi_P &= c \Psi_S, \\ c \left[\frac{\hbar}{m} \sigma_0 \tau_z \partial_x \Psi_P + i\alpha \cos \phi \sigma_z \tau_0 \Psi_P \right] &= \frac{\hbar}{m} \sigma_0 \tau_z \partial_x \Psi_S + \frac{\hbar \eta_\mu q}{m} \sigma_0 \tau_z \Psi_S + \frac{i\Delta}{k_F} \tau_x \sigma_\theta \Psi_S, \end{aligned} \quad (5)$$

where c is a real, dimensionless parameter characterizing the junction transparency, and q is a real parameter with dimensions of wavenumber, corresponding to the strength of a delta-function barrier near the junction on the superconducting side. Here, Ψ_P and Ψ_S are the wavefunctions on the p -wave magnet and superconductor sides of the junction, evaluated at $x = 0$ and $x = L$.

The parameter $\eta_u = 1$ at $x = 0$ and $\eta_u = -1$ at $x = L$. Physically, c represents the hopping strength of the bond connecting the p -wave magnet to the superconductor in an equivalent lattice model [31] and we set $c = 1$.

Scattering Eigenfunctions.— Translational symmetry along \hat{y} ensures that momentum along \hat{y} is conserved. The eigenfunction of the Hamiltonian for an s -spin electron incident from the left p -wave magnet at energy E and angle of incidence χ has the form $\Psi(x)e^{ik_y y}$, where $k_y = k_y(e, E, \chi)$ is obtained from Eq. (3) with $\gamma = 1$ and $-\pi/2 < \chi < \pi/2$. The spatial part $\Psi(x)$ is expressed as:

$$\Psi(x) = \begin{cases} e^{ik_{x,e,s}^i x} |e, s\rangle + \sum_{p,s'} r_{p,s',e,s} e^{ik_{x,p,s'}^l x} |p, s'\rangle, & \text{for } x < 0, \\ \sum_{j',j,\sigma} s_{j',j,\sigma} e^{\sigma i k_{x,j,\sigma} x} |\phi_{j',j,\sigma}\rangle, & \text{for } 0 < x < L, \\ \sum_{p,s'} t_{p,s',e,s} e^{ik_{x,p,s'}^r x} |p, s'\rangle, & \text{for } x > L, \end{cases} \quad (6)$$

where $k_{x,e,s}^i = k_x(e, E, \chi)$ for $\gamma = 1$, and $k_{x,p,s'}^l$ ($k_{x,p,s'}^r$) are the x -components of the wavenumber for left-moving (right-moving) p -type particles with spin s' in the regions $x < 0$ ($x > L$), calculated using the respective dispersion relation with the same choice of k_y . Here, when wavenumber of a particle ($k_{x,p,s'}^l$ or $k_{x,p,s'}^r$) becomes complex, the one that gives exponentially decaying wavefunction away from the junction is chosen out of two possible solutions. The spinors $|p, s\rangle$ are given by $|e, \uparrow\rangle = [1, 0, 0, 0]^T$, $|e, \downarrow\rangle = [0, 1, 0, 0]^T$, $|h, \uparrow\rangle = [0, 0, 1, 0]^T$, and $|h, \downarrow\rangle = [0, 0, 0, 1]^T$.

In the superconducting region, $k_x = \pm k_{x,j}$ ($j = 1, 2$) are the wavenumbers at energy E , obtained from the dispersion in Eq. (4). The corresponding eigenspinor $|\phi_{j',j,\sigma}\rangle$ is associated with $k_x = \sigma k_{x,j}$, where $\sigma = \pm 1$, and is doubly degenerate, as captured by the index $j' = 1, 2$. The scattering coefficients $r_{p,s',e,s}$, $s_{j',j,\sigma}$, and $t_{p,s',e,s}$ are unknowns that are determined using the boundary conditions in Eq. (5).

Conductivities.— Once the scattering coefficients are determined, local and nonlocal differential conductivities $G_{\mathcal{L}\mathcal{L}}$ and $G_{\mathcal{R}\mathcal{L}}$ can be calculated. The conductivities are given by

$$G_{\mathcal{L}\mathcal{L}} = \frac{e}{\hbar^2} m \int_{-\pi/2}^{\pi/2} d\chi [J_{x,\uparrow,\mathcal{L}}^c(\chi) + J_{x,\downarrow,\mathcal{L}}^c(\chi)]$$

$$G_{\mathcal{R}\mathcal{L}} = \frac{e}{\hbar^2} m \int_{-\pi/2}^{\pi/2} d\chi [J_{x,\uparrow,\mathcal{R}}^c(\chi) + J_{x,\downarrow,\mathcal{R}}^c(\chi)], \quad (7)$$

where $J_{x,s,\mathcal{L}/\mathcal{R}}^c$ are the charge current densities carried in the region $x < 0$ (\mathcal{L}) and $x > L$ (\mathcal{R}), when a spin- s electron is incident from the left. The currents on the left have the form $J_{x,s,\mathcal{L}}^c = e\hbar k_{0,e} \cos \chi / m + J_{x,s,\mathcal{L}}^{c,r}$, where the first term corresponds to current due to incident spin- s electron and the second term refers to the current due to

all reflected electrons and holes.

$$J_{x,s,\mathcal{L}}^{c,r} = e \sum_{p,s'} \left[\frac{\hbar k_{x,p,l,s'}}{m} + \eta_p \eta_s \alpha \cos \phi \right] |r_{p,s',e,s}|^2 \beta_{\mathcal{L},p,s'}, \quad (8)$$

where $\beta_{\mathcal{L},p,s'} = 1$ if $k_{x,p,l,s'}$ is purely real and zero otherwise. This is because, evanescent waves do not carry current in leads. In a similar way, the current on the right magnet is given by

$$J_{x,s,\mathcal{R}}^c = e \sum_{p,s'} \left[\frac{\hbar k_{x,p,r,s'}}{m} - \eta_p \eta_s \alpha \cos \phi \right] |t_{p,s',e,s}|^2 \beta_{\mathcal{R},p,s'}, \quad (9)$$

where $\beta_{\mathcal{R},p,s'} = 1$ if $k_{x,p,r,s'}$ is purely real and zero otherwise.

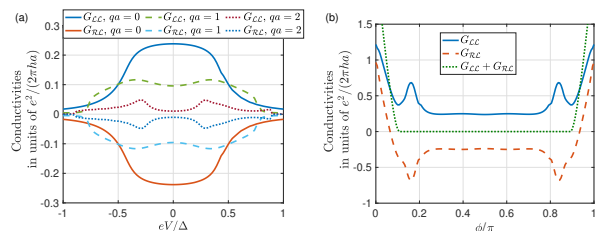


FIG. 3. Conductivities $G_{\mathcal{L}\mathcal{L}}$ and $G_{\mathcal{R}\mathcal{L}}$ versus: (a) bias V , (b) orientation angle ϕ . In (a), different curves are for different values of q - the barrier strength at the junction. Parameters: $\mu = -\mu_s$, $\alpha = 1.5\hbar/(ma)$, $\phi = \pi/2$, $\Delta = 0.1\mu_s$, $\theta = 0$ and $L = 5a$.

Results.— Parameters are expressed in units of m and μ_s , with $a = \hbar/\sqrt{m\mu_s}$ as the characteristic length scale. Setting $\mu = -\mu_s$, $\alpha = 1.5\hbar/(ma)$, $\phi = \pi/2$, $\Delta = 0.1\mu_s$, $\theta = 0$, and $L = 5a$, the conductivities $G_{\mathcal{L}\mathcal{L}}$ and $G_{\mathcal{R}\mathcal{L}}$ are calculated and plotted in Fig. 3 as functions of (a) the bias V and, (b) the orientation angle ϕ . For $\theta = 0$, the pairing occurs between electrons with the same spin oriented along $\pm \hat{z}$. Under these conditions, an incident electron from the left can either reflect back as an electron or transmit to the right as a hole via CAR, resulting in $G_{\mathcal{L}\mathcal{L}} = -G_{\mathcal{R}\mathcal{L}}$. For this to happen, the constant energy contours for the two spins need to be well separated (as in Fig. 2).

In Fig. 3(b), the conductivities are plotted as functions of ϕ with the bias fixed near zero. It is observed that in the range $0.11\pi < \phi < 0.89\pi$, the local and nonlocal conductivities sum-up to zero, indicating absence of Andreev reflection. Outside this range, same-spin electron-hole pairs with identical k_y exist on the left, enabling Andreev reflection. Additionally, same-spin electrons with the same k_y are present on both sides of the superconductor, allowing ET. As a result, the two conductivities no longer sum to zero, and the nonlocal conductivity becomes positive near $\phi = 0$, indicating that ET dominates over CAR.

As a function of the chemical potential μ of the p -wave magnet, the conductivities exhibit the behavior shown in

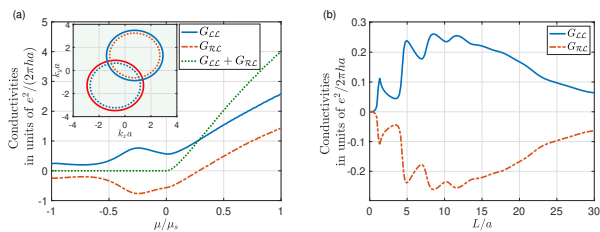


FIG. 4. Conductivities at zero bias versus: (a) μ - the chemical potential of the p -wave magnet for $q = 0$, (b) L - the length of the superconductor for $q = 0$. Inset of (a): Constant energy contours for $\mu = \mu_s$, $\phi = \pi/3$, $E = 0.25\mu_s$. Solid (dotted) line indicates electron (hole), and red (blue) color indicates spin- \uparrow (\downarrow). Other parameters same as in Fig. 3.

Fig. 4(a). For $\mu_s > 0$, the two conductivities do not sum to zero. This is due to the crossing of constant energy contours for the two spins on each p -wave magnet, as illustrated in the inset of Fig. 4(a), which allows for both Andreev reflection and ET. For chemical potentials $\mu > 0.283\mu_s$, the sum of the conductivities becomes positive, indicating the dominance of ET over CAR.

The dependence of the conductivities on the length L of the superconductor is also significant. Since CAR arises from electron-to-hole conversion within the superconductor, CAR initially increases as L grows from zero. However, beyond a certain length, the exponentially decaying wavefunctions in the superconductor reduce the probability of the converted hole reaching the other p -wave magnet. The oscillatory behavior in the conductivities results from the real part of the wavenumbers in the superconductor, producing Fabry-Pérot-type oscillations [17, 32]. For normal incidence, $k_{x1} = (1.4124 + 0.0707i)/a$, giving a decay length of $1/\text{Im}[k_{x1}] = 14a$, where the conductivity peaks. The oscillation period is approximately $\pi/\text{Re}[k_{x1}] = 2.22a$, consistent with the observed results.

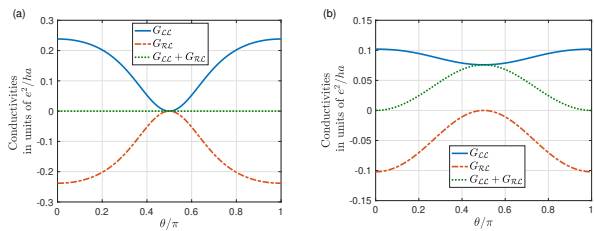


FIG. 5. Conductivities versus the angle θ between \hat{z} and the direction of spins that make equal spin triplet pairing in superconductor for (a) $V = 0$ and (b) $eV = 0.5\Delta$. $q = 0$ and other parameters same as in Fig. 3.

Next, we examine the dependence of the conductivities on the angle θ between the spins in the equal-spin triplet pairing of the superconductor and the easy axis \hat{z} of the p -wave magnet, as shown in Fig. 5. The magnitude of the nonlocal conductivity decreases as θ increases from

0 to $\pi/2$. At $\theta = \pi/2$, $G_{RL} = 0$ because the pairing is between electrons with opposite spins, and the spin component of the Cooper pair wavefunction takes the form $(|\uparrow\downarrow\rangle + |\downarrow\uparrow\rangle)$. In this case, for any incident electron on the left side, no corresponding hole of opposite spin exists on the right side.

Interestingly, at zero bias, $G_{LL} + G_{RL} = 0$, indicating the absence of Andreev reflection at the left interface. This occurs because the k_y values for the incident electrons are large, and for these values, no zero-energy bound states are present in the superconductor. However, this behavior changes at nonzero bias, where Andreev reflection contributes to transport for all $0 < \theta < \pi$, although ET is completely suppressed.

Summary and Outlook.— In this work, we studied the transport properties of a junction comprising p -wave magnets and a triplet superconductor, focusing on the interplay between crossed Andreev reflection (CAR) and electron tunneling (ET) as functions of key system parameters. For specific orientations of the p -wave magnets centered around $\phi = \pi/2$, CAR dominates, resulting in $G_{LL} + G_{RL} = 0$. Outside this range, the conductivities deviate from this condition due to the presence of same-spin electron-hole pairs on the same side or same spin electrons on two sides of the superconductor. The conductivities also exhibit a strong dependence on the chemical potential μ of the p -wave magnets, with ET overtaking CAR for larger μ . An essential condition for enhanced CAR is that the constant energy contours of the two spins in the p -wave magnet remain well-separated.

The length L of the superconductor significantly affects CAR, with an initial increase followed by suppression due to the decay of hole transmission for larger L , accompanied by Fabry-Pérot-type oscillations. Furthermore, the angle θ between the spin direction of the triplet pairing and the easy axis of the p -wave magnets plays a crucial role in transport. At $\theta = \pi/2$, the pairing involves opposite spins, completely suppressing CAR. These findings reveal a rich interplay of parameters that govern CAR and ET in p -wave magnet-triplet superconductor junctions. Materials such as CeNiAsO, predicted to exhibit p -wave magnetism [33], provide a promising platform for experimentally testing our predictions.

Acknowledgment.— The author acknowledges financial support from the ANRF (formerly SERB) Core Research Grant (CRG/2022/004311) and the University of Hyderabad Institute of Eminence PDF.

* abhirams@uohyd.ac.in

- [1] L. Šmejkal, A. B. Hellenes, R. González-Hernández, J. Sinova, and T. Jungwirth, Giant and tunneling magnetoresistance in unconventional collinear antiferromagnets with nonrelativistic spin-momentum coupling, Phys. Rev. X **12**, 011028 (2022).

- [2] L. Šmejkal, J. Sinova, and T. Jungwirth, Beyond conventional ferromagnetism and antiferromagnetism: A phase with nonrelativistic spin and crystal rotation symmetry, *Phys. Rev. X* **12**, 031042 (2022).
- [3] L. Šmejkal, J. Sinova, and T. Jungwirth, Emerging research landscape of altermagnetism, *Phys. Rev. X* **12**, 040501 (2022).
- [4] T. Jungwirth, R. M. Fernandes, J. Sinova, and L. Šmejkal, Altermagnets and beyond: Nodal magnetically-ordered phases, arXiv:2409.10034 (2024).
- [5] T. Jungwirth, R. M. Fernandes, E. Fradkin, A. H. MacDonald, J. Sinova, and L. Smejkal, From supefluid ^3He to altermagnets, arXiv:2411.00717 (2024).
- [6] P. Sukhachov and J. Linder, Impurity-induced friedel oscillations in altermagnets and p -wave magnets, *Phys. Rev. B* **110**, 205114 (2024).
- [7] A. A. Hedayati and M. Salehi, Transverse spin current at normal-metal $/p$ -wave magnet junctions, *Phys. Rev. B* **111**, 035404 (2025).
- [8] M. Ezawa, Purely electrical detection of the Néel vector of p -wave magnets based on linear and nonlinear conductivities, arXiv: 2410.21854 (2024).
- [9] P. Sukhachov, H. G. Giil, B. Brekke, and J. Linder, Coexistence of p -wave magnetism and superconductivity, arXiv:2412.14245 (2024).
- [10] S. Das, D. Suri, and A. Soori, Transport across junctions of altermagnets with normal metals and ferromagnets, *J. Phys.: Condens. Matter* **35**, 435302 (2023).
- [11] G. E. Blonder, M. Tinkham, and T. M. Klapwijk, Transition from metallic to tunneling regimes in superconducting microconstrictions: Excess current, charge imbalance, and supercurrent conversion, *Phys. Rev. B* **25**, 4515 (1982).
- [12] C. Sun, A. Brataas, and J. Linder, Andreev reflection in altermagnets, *Phys. Rev. B* **108**, 054511 (2023).
- [13] M. Papaj, Andreev reflection at the altermagnet-superconductor interface, *Phys. Rev. B* **108**, L060508 (2023).
- [14] K. Maeda, B. Lu, K. Yada, and Y. Tanaka, Theory of tunneling spectroscopy in unconventional p -wave magnet-superconductor hybrid structures, *J. Phys. Soc. Jpn.* **93**, 114703 (2024).
- [15] D. Beckmann, H. B. Weber, and H. v. Löhneysen, Evidence for crossed Andreev reflection in superconductor-ferromagnet hybrid structures, *Phys. Rev. Lett.* **93**, 197003 (2004).
- [16] T. Yamashita, S. Takahashi, and S. Maekawa, Crossed Andreev reflection in structures consisting of a superconductor with ferromagnetic leads, *Phys. Rev. B* **68**, 174504 (2003).
- [17] A. Soori and S. Mukerjee, Enhancement of crossed Andreev reflection in a superconducting ladder connected to normal metal leads, *Phys. Rev. B* **95**, 104517 (2017).
- [18] S.-B. Zhang and B. Trauzettel, Perfect crossed Andreev reflection in Dirac hybrid junctions in the quantum Hall regime, *Phys. Rev. Lett.* **122**, 257701 (2019).
- [19] R. Nehra, D. S. Bhakuni, A. Sharma, and A. Soori, Enhancement of crossed Andreev reflection in a Kitaev ladder connected to normal metal leads, *J. Phys.: Condens. Matter* **31**, 345304 (2019).
- [20] A. Soori, Transconductance as a probe of nonlocality of Majorana fermions, *J. Phys.: Condens. Matter* **31**, 505301 (2019).
- [21] M. F. Jakobsen, A. Brataas, and A. Qaiumzadeh, Electrically controlled crossed Andreev reflection in two-dimensional antiferromagnets, *Phys. Rev. Lett.* **127**, 017701 (2021).
- [22] A. Soori, Tunable crossed Andreev reflection in a heterostructure consisting of ferromagnets, normal metal and superconductors, *Solid State Commun.* **348-349**, 114721 (2022).
- [23] S.-C. Zhao, L. Gao, Q. Cheng, and Q.-F. Sun, Perfect crossed Andreev reflection in the proximitized graphene/superconductor/proximitized graphene junctions, *Phys. Rev. B* **108**, 134511 (2023).
- [24] S. Das and A. Soori, Crossed Andreev reflection in altermagnets, *Phys. Rev. B* **109**, 245424 (2024).
- [25] C. Benjamin, Crossed Andreev reflection as a probe for the pairing symmetry of ferromagnetic superconductors, *Phys. Rev. B* **74**, 180503 (2006).
- [26] F. Crépin, P. Buset, and B. Trauzettel, Odd-frequency triplet superconductivity at the helical edge of a topological insulator, *Phys. Rev. B* **92**, 100507 (2015).
- [27] P. Recher, E. V. Sukhorukov, and D. Loss, Andreev tunneling, coulomb blockade, and resonant transport of non-local spin-entangled electrons, *Phys. Rev. B* **63**, 165314 (2001).
- [28] A. Das, Y. Ronen, M. Heiblum, D. Mahalu, A. V. Kretinin, and H. Shtrikman, High-efficiency Cooper pair splitting demonstrated by two-particle conductance resonance and positive noise cross-correlation, *Nat. Commun.* **3**, 1165 (2012).
- [29] J. Schindele, A. Baumgartner, and C. Schönenberger, Near-unity Cooper pair splitting efficiency, *Phys. Rev. Lett.* **109**, 157002 (2012).
- [30] S. Russo, M. Kroug, T. M. Klapwijk, and A. F. Morpurgo, Experimental observation of bias-dependent non-local Andreev reflection, *Phys. Rev. Lett.* **95**, 027002 (2005).
- [31] A. Soori, Scattering in quantum wires and junctions of quantum wires with edge states of quantum spin Hall insulators, *Solid State Commun.* **360**, 115034 (2023).
- [32] S. K. Sahu and A. Soori, Fabry-Pérot interference in Josephson junctions, *Eur. Phys. J. B* **96**, 115 (2023).
- [33] A. B. Hellenes, T. Jungwirth, R. Jaeschke-Ubiergo, A. Chakraborty, J. Sinova, and L. Smejkal, p -wave magnets, arXiv:2309.01607 (2023).